Int. J. Heat Mass Transfer. Vol. 32, No. 11, pp. 2199–2207, 1989
Printed in Great Britain

0017-9310/89 $3.00 + 0.00

Periodic laminar convection in a tall vertical cavity

H. Q. YANG,† K. T. YANG and Q. XIA
Department of Aerospace and Mechanical Engineering, University of Notre Dame, IN 46556, U.S.A.

(*Received* 6 *September* 1988 *and in final form* 27 *March* 1989)

Abstract—The response of the flow in a tall vertical cavity to periodic surface temperature variations is studied analytically and numerically. At both low and high frequency limits, the response characteristics agree with those of natural convection along a vertical plate undergoing surface temperature oscillation. The effects of low and high Prandtl numbers and that of Rayleigh numbers at intermediate frequencies are also discussed.

INTRODUCTION

THIS PAPER describes a study of natural convection in a vertical tall cavity due to periodic heating on the vertical surfaces. One of the applications is the flow in double glazed windows due to cyclic temperature variations in the surroundings. It also finds application in energy systems where fluid motion may be initiated due to the periodic surface heating, even though the time average of the surface temperature or surface heat flux may be zero. A similar problem dealing with natural-convection boundary layers along a vertical plate due to surface temperature oscillation was studied by means of a linearized theory [1]. Asymptotic series solutions for low and high frequency ranges were formally obtained, from which response characteristics in velocity and temperature profiles as well as in the local rate of heat transfer at the plate are derived. It is found that in the low frequency solution, the first approximation is given by the quasi-steady-state solution, while for the high frequency range the leading terms are those of the shear-wave solution. On the other hand, studies on natural convection in cavities so far, as reviewed in refs. [2–4], deal very little with transient processes, which could be important in some instances, since the internal dynamics of the flow field in a cavity is sensitive to changes in the Rayleigh number. In general, the transient behavior of the flow field may be due to a step change in the temperature on the boundary wall [5, 6], oscillations from the inherent instability [7] and special temperature distribution imposed on the boundaries [8, 9]. Patterson and Imberger [10] have performed an ordering analysis for shallow cavities to delineate the condition under which the approach to steady state is oscillatory. The experiments by Yewell *et al.* [11], however, displayed no evidence of this oscillatory approach. Patterson [12] further clarified that the oscillatory behaviors also depended on the aspect ratio, and showed that the experiments of ref. [11] supported the scaling analysis of ref. [10]. The purpose of the present paper is to reveal the characteristics of the periodic flow and heat transfer behaviors in a tall vertical cavity at various imposed frequencies, and Rayleigh and Prandtl numbers.

FORMULATION AND ANALYSIS

We consider a tall two-dimensional cavity as shown in Fig. 1 with the Boussinesq approximation and the assumptions of constant properties and negligible flow work and viscous dissipation. The following dimensionless governing equations are applicable:

$$u_{,x}+v_{,y}=0 \tag{1}$$

$$u_{t}+uu_{,x}+vu_{,y}=-p_{,x}+Pr(u_{,xx}+u_{,yy}) \tag{2}$$

$$v_{t}+uv_{,x}+vv_{,y}=-p_{,y}+Pr(v_{,xx}+v_{,yy})+Pr\,Ra\,T \tag{3}$$

$$T_{t}+uT_{,x}+vT_{,y}=T_{,xx}+T_{,yy} \tag{4}$$

where the symbols are defined in the Nomenclature.

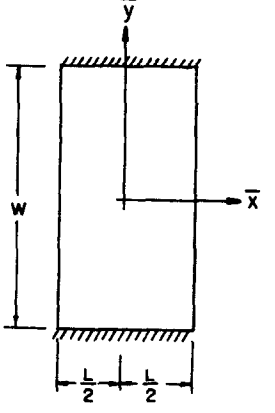

FIG. 1. Vertical cavity geometry.

† Presently with CFD Research Corporation, Huntsville, AL 35805, U.S.A.

NOMENCLATURE

$a_1, \ldots, a_6$	imaginary and real parts of a complex function	Re	real part of a complex function
A_y	aspect ratio, W/L	T	temperature
f	frequency	t	time variable
g_r	gravitational acceleration	u, v	velocity components
g, h, q	complex functions for temperature, velocity, and heat transfer, respectively	x, y	Cartesian coordinates
		W	height of cavity
		z	complex variable, $(1+\mathrm{i})/2^{1/2}$.
G, H, Q	functions for temperature, velocity, and heat transfer, respectively	Greek symbols	
		α	thermal diffusivity
Im	imaginary part of a complex function	β	volumetric expansion coefficient
k	thermal conductivity	$\theta_1, \ldots, \theta_3$	phase shift
L	length of cavity	μ	dynamic viscosity
Nu	Nusselt number	ρ	density.
p	static pressure		
Pr	Prandtl number, $\mu/(\rho\alpha)$	Superscript	
Ra	Rayleigh number, $\rho g_r \beta(\bar{T}_1 - \bar{T}_0)L^3/(\mu\alpha)$	$\bar{}$	dimensional quantities.

Here, velocities (u, v) are normalized by α/L; length by L; time by L^2/α; pressure by $\rho(\alpha/L)^2$; and temperature difference by $(\bar{T}_1 - \bar{T}_0)$. Here $(\bar{T}_1 - \bar{T}_0)$ is the amplitude of the surface temperature variation, and T_0 the base temperature. The non-slip condition holds for velocities on the walls. The top and bottom walls are taken as adiabatic. At the right-hand side wall of $\bar{x} = L/2$ (Fig. 1), a sinusoidal function of temperature is applied, i.e.

$$(\bar{T} - \bar{T}_0) = (\bar{T}_1 - \bar{T}_0)\sin(2\pi f t) \tag{5}$$

or

$$T = \sin(2\pi f t) \tag{6}$$

where f is a dimensionless frequency, defined by

$$f = \bar{f}L^2/\alpha. \tag{7}$$

On the left-hand side wall at $x = -1/2$, the thermal boundary condition can be either adiabatic or a prescribed temperature. In the present study, a sinusoidal function of temperature is also imposed, but with a 180° phase lag, i.e.

$$T = -\sin(2\pi f t). \tag{8}$$

The initial condition is that of stagnant flow and uniform temperature

$$t = 0, \quad u(x, y) = 0, \quad v(x, y) = 0, \quad T(x, y) = 0. \tag{9}$$

The solutions to the above set of equations and the corresponding boundary conditions can be obtained numerically, as will be shown in the next section. However, aside from the region near the horizontal walls, the flow in a vertical cavity with large aspect ratios and small Rayleigh number can be approximated as parallel in that v and T are both functions of x only, so that

$$u = 0, \quad v = v(x), \quad T = T(x) \tag{10}$$

and v and T are given by the solution to

$$v_t = Pr\, v_{,xx} + Pr\, Ra\, T \tag{11}$$

$$T_t = T_{,xx}. \tag{12}$$

The steady-state solution of parallel flow at both very high aspect ratios ($A_y \gg 1$) and low aspect ratios ($A_y \ll 1$) has been reviewed by Simpkins and Chen [13] for the application of crystal growth, and some studies on natural convection in a tall cavity related to the transition from the conduction regime to the boundary layer regime are also available [14–16].

The normal-mode solution of equation (12) subject to boundary conditions (6) and (8) is simply

$$T = \mathrm{Im}[g(x)\exp(\mathrm{i}2\pi f t)] \tag{13}$$

where $g(x)$ is a complex function given by

$$g(x) = \sinh[zx(2\pi f)^{1/2}]/\sinh[z/2(2\pi f)^{1/2}] \tag{14}$$

and Im represents the imaginary part of the function. Also

$$z = (1+\mathrm{i})/2^{1/2}. \tag{15}$$

Substitution of T into equation (11) yields a solution for the velocity v as

$$v = \mathrm{Im}[h(x)\exp(\mathrm{i}2\pi f t)] \tag{16}$$

where

$$h(x) = \frac{Ra}{\mathrm{i}2\pi f(1/Pr - 1)}\left\{\frac{\sinh[zx(2\pi f)^{1/2}]}{\sinh[z/2(2\pi f)^{1/2}]} - \frac{\sinh[zx(2\pi f/Pr)^{1/2}]}{\sinh[z/2(2\pi f/Pr)^{1/2}]}\right\}. \tag{17}$$

The Nusselt number, which represents the heat flux supplied or withdrawn from the wall, can be defined as

$$Nu = k(\bar{T}_{,\bar{x}})_{\bar{x}=L/2}/[k(\bar{T}_1-\bar{T}_0)/L] = (T_{,x})_{x=1/2} = \mathrm{Im}\,[q(f)\exp(\mathrm{i}2\pi ft)] \quad (18)$$

where

$$q(f) = \{z(2\pi f)^{1/2}\coth[z/2(2\pi f)^{1/2}]\}. \quad (19)$$

By separating the real and imaginary parts, the above solutions can be conveniently written in the following more explicit forms:

$$T = G(x,f)\sin(2\pi ft+\theta_1) \quad (20)$$

$$v = H(x,f,Pr,Ra)\sin(2\pi ft+\theta_2-\pi/2) \quad (21)$$

$$Nu = Q(f)\sin(2\pi ft+\theta_3-\pi/4) \quad (22)$$

where

$$G(x,f) = [(a_1)^2+(a_2)^2]^{1/2} \quad (23)$$

$$H(x,f,Pr,Ra) = Ra[(a_1-a_3)^2+(a_2-a_4)^2]^{1/2}/[2\pi f(1/Pr-1)] \quad (24)$$

$$Q(f) = (2f)^{1/2}[(a_5)^2+(a_6)^2]^{1/2} \quad (25)$$

and

$$\theta_1 = \tan^{-1}(a_2/a_1) \quad (26)$$

$$\theta_2 = \tan^{-1}[(a_2-a_4)/(a_1-a_3)] \quad (27)$$

$$\theta_3 = \tan^{-1}(a_6/a_5) \quad (28)$$

$$a_1 = \mathrm{Re}\{\sinh[zx(2\pi f)^{1/2}]/\sinh[z/2(2\pi f)^{1/2}]\} \quad (29)$$

$$a_2 = \mathrm{Im}\{\sinh[zx(2\pi f)^{1/2}]/\sinh[z/2(2\pi f)^{1/2}]\} \quad (30)$$

$$a_3 = \mathrm{Re}\{\sinh[zx(2\pi f/Pr)^{1/2}]/\sinh[z/2(2\pi f/Pr)^{1/2}]\} \quad (31)$$

$$a_4 = \mathrm{Im}\{\sinh[zx(2\pi f/Pr)^{1/2}]/\sinh[z/2(2\pi f/Pr)^{1/2}]\} \quad (32)$$

$$a_5 = \mathrm{Re}\{\coth[z/2(2\pi f)^{1/2}]\} \quad (33)$$

$$a_6 = \mathrm{Im}\{\coth[z/2(2\pi f)^{1/2}]\}. \quad (34)$$

Here Re represents the real part of a complex function. All the a's can be easily determined through the relation

$$\sinh(x+\mathrm{i}y) = \sinh(x)\cos(y)+\mathrm{i}\cosh(x)\sin(y). \quad (35)$$

It is to be noted that the temperature and the velocity are anti-symmetric with respect to $x = 0$ so that at any y

$$\int_{-1/2}^{1/2} v\,\mathrm{d}x = 0. \quad (36)$$

It is also clear that the quantities θ_1, $(\theta_2-\pi/2)$ and $(\theta_3-\pi/4)$ represent the respective phase shifts of the temperature T, velocity v and Nu oscillations relative to that of the imposed surface temperature at $x = 1/2$.

RESULTS OF LIMITING ANALYSIS AND NUMERICAL COMPUTATIONS

To reveal the characteristics of the periodic flow and heat transfer, several limiting cases can first be considered, and results of numerical computations without imposing the parallel flow condition are then given in terms of detailed flow structure and the thermal field.

Limiting cases

(1) $f \to 0$. If the frequency of the forcing function is vanishingly small, a limit exists and leads to the following simplified expressions for the temperature, velocity and heat transfer:

$$T = 2x\sin(2\pi ft) \quad (37)$$

$$v = Ra/3[1/4-(x)^2]x\sin(2\pi ft) \quad (38)$$

$$Nu = 2\sin(2\pi ft). \quad (39)$$

As seen from the above expressions, the flow, temperature and heat transfer rate are all in phase with the surface temperature oscillations. It is also interesting to see that the flow field is independent of the Prandtl number. This can be easily understood from the point that for small f, the transient terms in equations (11) and (12) are insignificant so that the solutions are simply the steady-state solutions based on the instantaneous boundary temperature difference. This result agrees with the quasi-steady solution in ref. [1] for natural convection along a vertical plate undergoing surface temperature oscillation.

(2) $f \to \infty$. When the frequency is very high, in contrast to the small frequency case, the transient terms in equations (11) and (12) become dominant, resulting in phase shifts in the temperature and velocity responses. By taking the limit, we have the temperature solution for $1/2 > x > 0$ (for $0 > x > -1/2$, they are anti-symmetrical) given by

$$T = \exp[-(1/2-x)(\pi f)^{1/2}]\times\sin[2\pi ft-(1/2-x)(\pi f)^{1/2}] \quad (40)$$

and for v, the solution is still the same as that in equation (21) except that the coefficients are simplified to

$$a_1 = \exp[-(1/2-x)(\pi f)^{1/2}]\times\cos[-(1/2-x)(\pi f)^{1/2}] \quad (41)$$

$$a_2 = \exp[-(1/2-x)(\pi f)^{1/2}]\times\sin[-(1/2-x)(\pi f)^{1/2}] \quad (42)$$

$$a_3 = \exp[-(1/2-x)(\pi f/Pr)^{1/2}]\times\cos[-(1/2-x)(\pi f/Pr)^{1/2}] \quad (43)$$

$$a_4 = \exp[-(1/2-x)(\pi f/Pr)^{1/2}] \times \sin[-(1/2-x)(\pi f/Pr)^{1/2}] \quad (44)$$

$$Nu = (2\pi f)^{1/2} \sin(2\pi ft - \pi/4). \quad (45)$$

These results are typically those of shear waves and the amplitude decays exponentially away from the surface. At any point $(1/2-x)$, the phase shift in the temperature is given by

$$\theta_1 = (1/2-x)(\pi f)^{1/2}. \quad (46)$$

The heat transfer rate here increases with the square root of the frequency and realizes a $\pi/4$ phase shift relative to the surface temperature. The instantaneous heat flux supplied or withdrawn from the surfaces may be significant at such high frequency situations. These results again agree with that of the vertical plate boundary layers analyzed in ref. [1].

(3) $Pr \to 0$. Since the temperature field is decoupled from the velocity, the variation of the Prandtl number only results in a change of the velocity field. When Pr is small, H becomes

$$H(x, f, Pr, Ra) = Pr\, Ra[(a_1-a_3)^2 + (a_2-a_4)^2]^{1/2}/(2\pi f) \quad (47)$$

and a_3 and a_4 are given by (for $0 \leqslant x \leqslant 1/2$)

$$a_3 = \exp[-(1/2-x)(\pi f/Pr)^{1/2}] \times \cos[-(1/2-x)(\pi f/Pr)^{1/2}] \quad (48)$$

$$a_4 = \exp[-(1/2-x)(\pi f/Pr)^{1/2}] \times \sin[-(1/2-x)(\pi f/Pr)^{1/2}]. \quad (49)$$

It is seen that a_3 and a_4 are important only in the regions near the wall (small $(1/2-x)$). Away from the wall, the flow field shows the same characteristics as those for the temperature field, but with a $\pi/2$ phase shift relative to the temperature field. The amplitude of the flow is proportional to the Prandtl number, and can be very small at low Prandtl numbers.

(5) $Pr \to \infty$. At large Prandtl numbers, H is given by

$$H = Ra[(a_1-a_3)^2 + (a_2-a_4)^2]^{1/2}/(2\pi f) \quad (50)$$

where

$$a_3 = 2x, \quad a_4 = 0. \quad (51)$$

Now in the region away from the walls (small x), the flow field still shows the same characteristics as the temperature, but the amplitude of the flow oscillation is independent of Prandtl number, as a result of the balance between the viscous and buoyancy forces. This is a typical result found in the cavity flow containing fluid at high Prandtl numbers.

Numerical computations and comparison

(1) $Pr = 0.7$ and 7.0. The functions G, H and Q, as well as θ_1, θ_2 and θ_3 given previously determine the basic features of the heat transfer and fluid flow responses at any combination of the parameters Pr, Ra, f and x. Due to the fact that the energy transport is by conduction only, the functions $G(x, f)$, Q, θ_1 and θ_3 are well known and fully documented [17]. Our attention now is directed to functions H and θ_2. In Fig. 2 the function H is depicted for Prandtl numbers of 0.7 and 7.0. For both Prandtl numbers, as predicted from equation (38), the distribution of H with respect to x is that of a cubic function when frequencies are relatively low. The magnitude of H, however, decreases with an increase in frequency. When the frequency is high, H shows the characteristics of a shear layer in that the local maximum of H shifts to the region near the wall, and H drops exponentially to the center of the cavity. In Fig. 3 the phase shifts

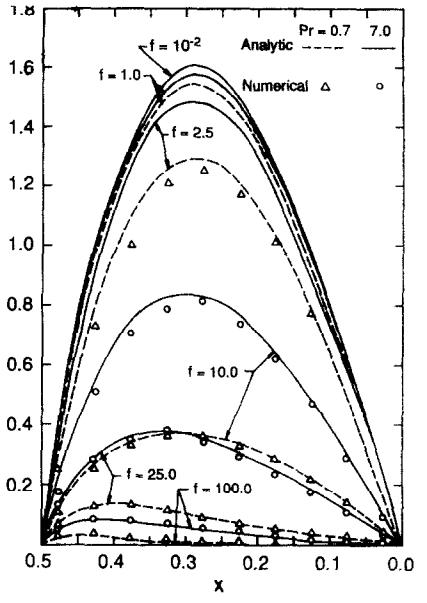

FIG. 2. Function $H(x)$ at $Ra = 10^2$, $Pr = 0.7$ and 7.0 and various frequencies.

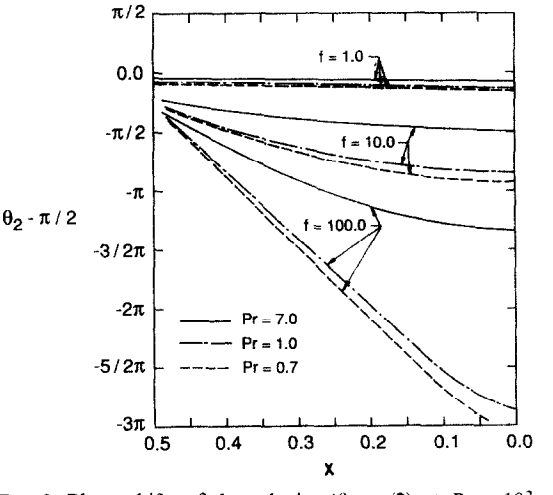

FIG. 3. Phase shifts of the velocity $(\theta_2-\pi/2)$ at $Ra = 10^2$, $Pr = 0.70$, 1.0 and 7.0, and various frequencies.

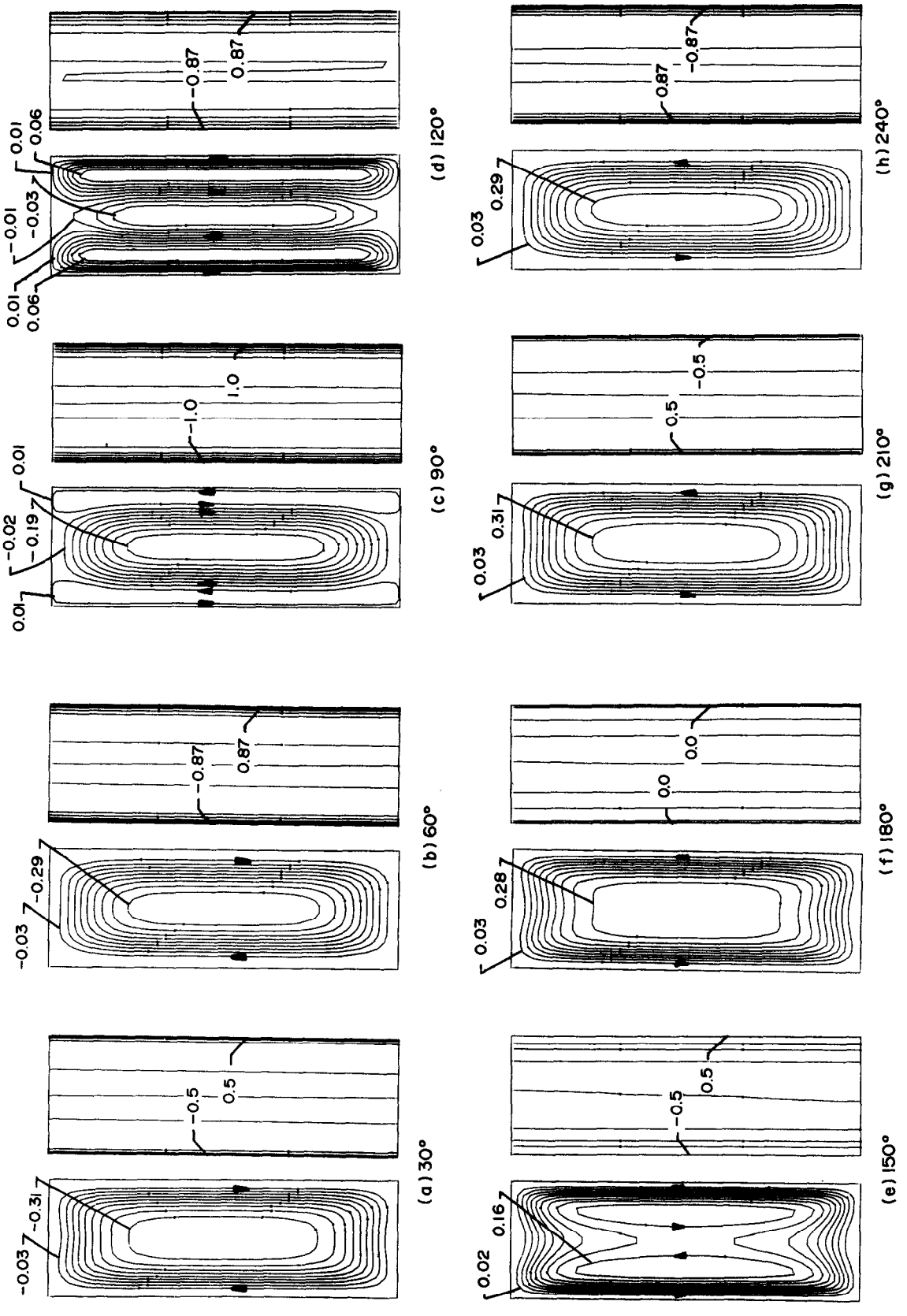

FIG. 4. Streamlines and isotherms at $Ra = 10^3$, $f = 50$ and $Pr = 7.0$.

$(\theta_2-\pi/2)$ for the Prandtl numbers of 0.7, 1.0 and 7.0 are displayed. The velocities at low frequencies are seen all in phase across the cavity. The phase shifts at different x become significant at high frequencies, especially for the fluid with the lower Prandtl number. This phenomenon can be interpreted by that, for $Pr < 1.0$, the buoyancy term in the momentum equation (11) is balanced by the transient term, while for $Pr > 1.0$ it is balanced by the viscous term.

The numerical calculations by the finite difference method for the original equations (1)–(4) have also been carried out to reveal the detailed flow structure and the temperature field, as well as the influence of Rayleigh number, including the effects of the top and bottom adiabatic walls. The numerical procedure is by the control volume finite-difference approach, and the convective terms are discretized by the QUICK scheme. The validation, and grid refinement studies have been described in ref. [18], and hence will not be repeated here. The calculations start from the stagnant flow condition, and the results are obtained after the periodic flows are established. The time step sizes are such that 360 time steps cover one cycle of the oscillation. In the calculations a 20×40 cell system is adopted with an aspect ratio A_y (W/L) of 3.0. In Fig. 2 the numerically calculated H at $y = 0$ with several frequencies are also depicted and generally good agreement with the corresponding limiting analytical solutions is found. Deviations of numerical results from the quasi-steady solution at lower frequencies come from the tall cavity approximation, where the effect of the upper and lower boundaries comes into play. In Fig. 4 the streamlines and isotherms from the numerical computations are plotted to show the flow and temperature fields at a Prandtl number of 7.0. The angles marked are those of the forcing function at $x = 1/2$. The instantaneous temperatures on the walls are marked on the isotherms for comparison with the flow responses. At a 30° phase angle of the forcing function, the fluid motion as seen from Fig. 4(a) is contrary to the buoyancy driven flow in that the fluid flows down along the hot wall, and up along the cold wall. This indicates clearly the phase shift of the responses of the velocity field. At an angle of 60°, the buoyancy becomes stronger, and the out-of-phase motion (clockwise circulation) gets weaker as indicated by the stream-function values. Up to an angle of 90° the original motion persists, and two cells driven by buoyancy appear along the cold and hot walls. A phase lag of about 90° is observed in this situation, which agrees with the analytical prediction from Fig. 3. The clockwise motion becomes smaller at an angle of 120° of the forcing function, and two buoyancy driven cells grow to a relatively large size, and finally combine to a complete circulation at 150° and 180°. The motions at 210° and 240° are similar to the ones at 30° and 60°, except they are out of phase here. From these temperature and velocity fields, the generation, regrouping and disappearance of the convection cells in the cavity, as well as the delay of the response of the flow field can be clearly visualized.

(2) Influence of the Rayleigh number. As noted above, the normal-mode analysis is for conduction dominant heat transfer, and there is no convection effect in equation (12). Therefore, it is suited only for the low Rayleigh number range. It remains to examine the significance of higher Rayleigh numbers in the present problem. This is done by means of numerical computations. In Fig. 5 the function (H/Ra), which should be independent of Ra according to equation (24), is shown for $Pr = 0.7$ and $f = 25.0$ at various Rayleigh numbers. It is interesting to see that the magnitude of H/Ra increases with an increase of Rayleigh number at first, which implies an initiation of the convective heat transfer. Up to a certain Ra (about 10^4 here), the magnitude of H/Ra starts to decrease and changes its characteristics to those of boundary layers. This can be understood by noting that, when the Rayleigh number increases to a certain value, flow transition from conduction dominant mechanism to the convection dominant mechanism occurs, so that finally it is of the boundary layer type. In the boundary

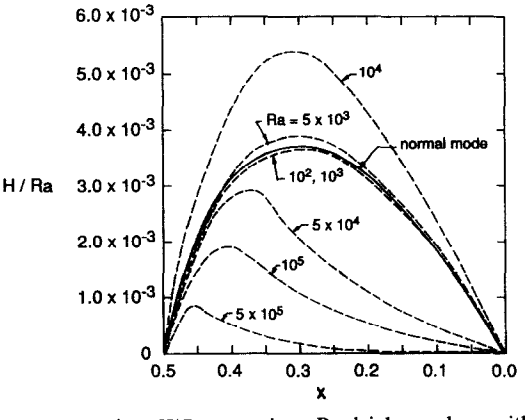

FIG. 5. Function H/Ra at various Rayleigh numbers with $Pr = 0.7$ and $f = 25.0$.

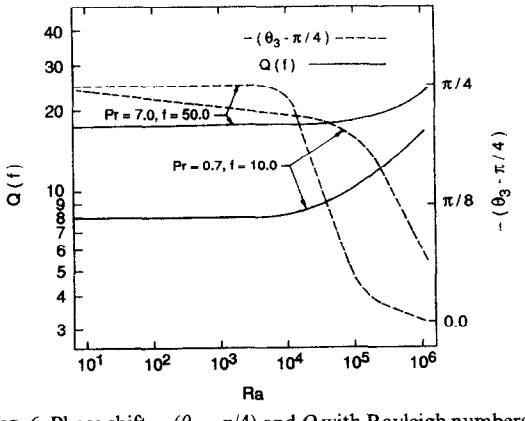

FIG. 6. Phase shift $-(\theta_3-\pi/4)$ and Q with Rayleigh numbers at $Pr = 0.7$ and $f = 10$, and $Pr = 7.0$ and $f = 50$.

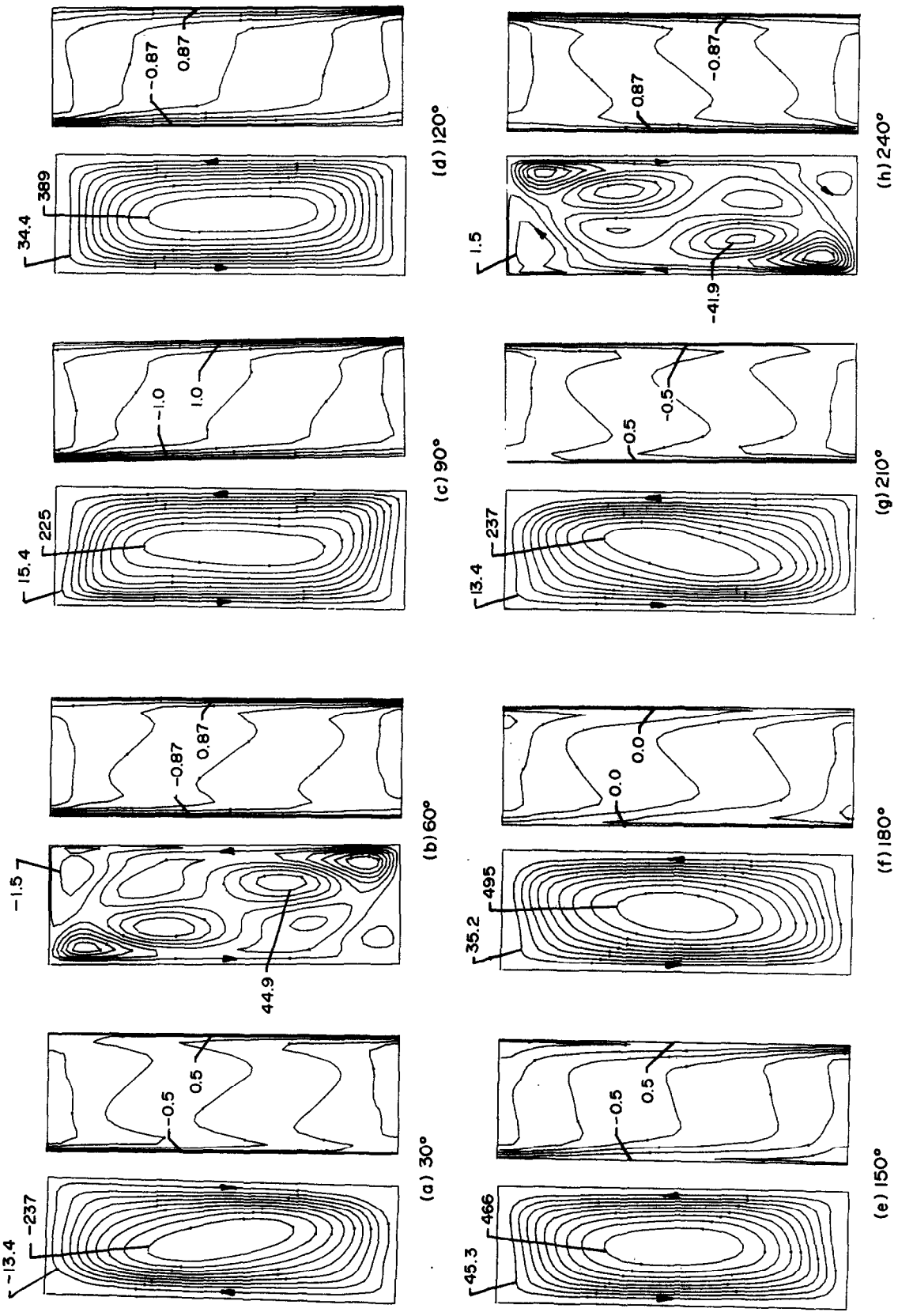

FIG. 7. Streamlines and isotherms at $Ra = 10^5$, $f = 50$ and $Pr = 7.0$.

layer flow the velocity should be scaled by $Ra^{1/2}$ instead of Ra [3, 4]. If $H/Ra^{1/2}$ is plotted against x, a monotonic increase of the amplitude with Ra can be found.

The heat transfer rate Q and the phase shift θ_3 are shown in Fig. 6. The amplitude of the heat transfer rate Q is seen to increase with Ra due to the convection effect, while the phase shift starts from $\pi/4$ (as for high frequency), rapidly drops to about 0° after the flow becomes that of the boundary layers. The flow structures at $Ra = 10^5$, $Pr = 7.0$ and $f = 50$ are given in Fig. 7. On comparing those in Fig. 4 with $Ra = 10^3$, it is shown clearly that the flow in the cavity is of the boundary layer type with isotherms accumulating near the walls and stratifying in the core. Also, despite similar changes of the convection cells over the oscillation cycle, the cell structures are now much more complex and the number of cells in the multi-cell structure is greatly increased. The corresponding Q and θ_3 for the above case are also given in Fig. 6. A further increase in Rayleigh number may result in additional internal flow oscillations [6]. The complicated interaction between the external forcing function and the internal unsteadiness is beyond the scope of the present study.

CONCLUDING REMARKS

The response of the flow in a tall vertical cavity to periodic surface temperature variations is studied analytically and numerically. Analytical closed-form results are obtainable under the parallel-flow conditions and heat transfer across the cavity is by conduction only. These results are valid in the limiting cases of either very large aspect ratios or low Rayleigh numbers. For high Rayleigh numbers, results in the flow and temperature fields have been obtained by finite-difference calculations for a cavity with an aspect ratio of 3.0. The following conclusions can be drawn.

(1) For large aspect ratios or low Rayleigh numbers, the low-frequency limit is given by the quasi-steady solution and the high-frequency limit is that of the shear-wave solution, and these results are identical to those of natural convection along a vertical plate undergoing surface-temperature oscillation.

(2) Numerical finite-difference solutions have also been carried out for a cavity with an aspect ratio of 3.0 over a range of Rayleigh numbers up to 5×10^5 and frequencies up to $f = 50$ at Prandtl numbers of 0.7 and 7.0. Results in the temperature field agree with those of the analytical solutions under parallel-flow conditions at Rayleigh numbers below 10^3. At higher Rayleigh numbers, the effects of the adiabatic horizontal surfaces become increasingly more apparent.

(3) In the conduction-dominant regime at low Rayleigh numbers, the flow patterns, however, are distinctly different from those of the analytical solutions due to the presence of the horizontal surfaces. Within a cycle of the surface temperature oscillation at $Ra = 10^2$ and $Pr = 7.0$, the flow in the cavity undergoes transitions from unicell to three-cell structures, and then back to the unicell flow pattern. On the other hand, at the midheight of the cavity, the flow velocities are essentially parallel.

(4) As the Rayleigh number increases, convection begins to change the conduction-dominant behavior in the cavity at about $Ra = 10^4$ in the ranges of Prandtl numbers and frequencies considered. The formation of boundary layers is clearly seen even at a Rayleigh number of 5×10^4. At $Ra = 10^5$, the flow is distinctly convection dominated. The corresponding streamline and isotherm plots also show respectively the transitions of unicell and multi-cell to unicell flow patterns, the thermal boundary layers and the stratified core, even though the multi-cell flow structure is now much more complex and the number of cells is greatly increased.

Our current continuing studies of cavity-flow responses to surface temperature oscillations address smaller aspect ratios including that of a square cavity, and the results will be reported at a future date.

REFERENCES

1. M. D. Kelleher and K. T. Yang, Heat transfer response of laminar free-convection boundary layers along a vertical plate to surface-temperature oscillations, *Z. Angew Math. Phys.* **19**, 31–44 (1968).
2. I. Catton, Natural convection in enclosures. In *Heat Transfer 1978*, Vol. 6, pp. 13–43. Hemisphere, Washington, DC (1978).
3. S. Ostrach, Natural convection heat transfer in cavity and cells. In *Heat Transfer 1982*, Vol. 1, pp. 365–379. Hemisphere, Washington, DC, (1982).
4. K. T. Yang, Natural convection in enclosures. In *Handbook of Single Phase Convective Heat Transfer* (Edited by K. Kakac, R. K. Shah and W. Aung), Chap. 13. Wiley-Interscience, New York (1987).
5. V. F. Nicolette, K. T. Yang and J. R. Lloyd, Transient cooling by natural convection in a two-dimensional square enclosure, *Int. J. Heat Mass Transfer* **28**, 1721–1732 (1985).
6. Y. S. Lin, An experimental study of flow patterns and heat transfer by natural convection inside cubic enclosure, Master's thesis, Kansas State University (1982).
7. D. G. Briggs and D. N. Jones, Two-dimensional periodic natural convection in a rectangular enclosure of aspect ratio one, *J. Heat Transfer* **107**, 850–854 (1985).
8. K. Kitamura, K. Komiama and T. Sato, Oscillatory convection in rectangular cavity, *Bull. J.S.M.E.* **27**, 2463–2469 (1984).
9. D. Poulikakos, Natural convection in a confined fluid-filled space driven by a single vertical wall with warm and cold regions, *J. Heat Transfer* **107**, 867–876 (1985).
10. J. C. Patterson and J. Imberger, Unsteady natural convection in a rectangular cavity, *J. Fluid Mech.* **100**(1), 65–86 (1980).
11. R. Yewell, D. Poulikakos and A. Bejan, Transient natural convection experiments in shallow enclosures, *J. Heat Transfer* **104**, 535–538 (1982).
12. J. C. Patterson, On the existence of an oscillatory approach to steady natural convection in cavities, *J. Heat Transfer* **106**, 104–108 (1984).
13. P. G. Simpkins and K. S. Chen, Natural convection

in horizontal containers with applications to crystal growth. In *Natural Convection Fundamentals and Applications* (Edited by S. Kakac, W. Aung and R. Viskanta), pp. 1010–1032. Hemisphere, Washington, DC (1985).
14. S. A. Korpela, A study on the effect of Prandtl number on the stability of the conduction regime of natural convection in an inclined slot, *Int. J. Heat Mass Transfer* **17,** 215–222 (1974).
15. R. F. Bergholtz, Instability of steady natural convection in a vertical layer, *J. Fluid Mech.* **84,** 743–768 (1978).
16. S. A. Korpela, Y. Lee and J. E. Drummond, Heat transfer through a double window, *J. Heat Transfer* **104,** 539–544 (1982).
17. H. S. Carslaw and J. C. Jaeger, *Conduction of Heat in Solids*. Clarendon Press, Oxford (1959).
18. H. Q. Yang, K. T. Yang and J. R. Lloyd, Laminar natural convection flow transition in tilted three-dimensional longitudinal rectangular enclosures, *Int. J. Heat Mass Transfer* **30,** 1637–1644 (1987).

CONVECTION LAMINAIRE PERIODIQUE DANS UNE CAVITE VERTICALE ET HAUTE

Résumé—On étudie analytiquement et numériquement la réponse de l'écoulement, dans une cavité verticale et haute, à des variations périodiques de température de la surface. A la fois pour les limites de fréquence basse et élevée, les caractéristiques de réponse s'accordent avec celles de la convection naturelle le long d'une plaque verticale soumise à une oscillation de température de surface. Les effets des nombres de Prandtl faibles ou élevés sont discutés ainsi que ceux des nombres de Rayleigh à des fréquences intermédiaires.

PERIODISCHE LAMINARE KONVEKTION IN EINEM HOHEN VERTIKALEN HOHLRAUM

Zusammenfassung—Die Antwort der Strömung in einem hohen vertikalen Hohlraum auf periodische Veränderungen der Oberflächentemperatur wird analytisch und numerisch untersucht. Sowohl bei der unteren als auch bei der oberen Grenzfrequenz stimmen die Antwortcharakteristiken mit denen einer natürlichen Konvektionsströmung entlang einer vertikalen Platte, die periodischen Veränderungen der Oberflächentemperatur unterworfen ist, überein. Der Einfluß niedriger und hoher Prandtl-Zahlen und derjenige der Rayleigh-Zahl bei mittleren Frequenzen wird ebenfalls behandelt.

ПЕРИОДИЧЕСКАЯ ЛАМИНАРНАЯ КОНВЕКЦИЯ В ВЕРТИКАЛЬНОЙ ПОЛОСТИ БОЛЬШОЙ ВЫСОТЫ

Аннотация—Аналитически и численно исследуется влияние периодических изменений температуры поверхности на течение в вертикальной полости большой высоты. Как в высокочастотном, так и в низкочастотном пределе характеристики процесса согласуются с соответствующими характеристиками при естественной конвекции у вертикальной пластины с температурными колебаниями на ее поверхности. Обсуждаются также предельные случаи низких и высоких значений чисел Прандтля и Рэлея при промежуточных частотах.